Sustainability **2015**, *7*, 11190-11212; doi:10.3390/su70811190

OPEN ACCESS

sustainability

ISSN 2071-1050

www.mdpi.com/journal/sustainability

Article

Scaled Experimental Study on Maximum Smoke Temperature along Corridors Subject to Room Fires

Zheli Xing [1], Jinfeng Mao [1,*], Yuliang Huang [1], Jin Zhou [1], Wei Mao [2] and Feifan Deng [1]

[1] Institute of Military Environmental Teaching and Research, PLA University of Science and Technology, Nanjing 210007, China; E-Mails: zheli86@sina.com (Z.X.); yulianghuang84@sina.com (Y.H.); mingmeng.2006@163.com (J.Z.); dengfeifanstudy@sina.com (F.D.)

[2] The 4th Design and Research Institute of Engineering Corps, Beijing 100850, China; E-Mail: morewell@sina.com

* Author to whom correspondence should be addressed; E-Mail: maojinfeng628@sina.com; Tel./Fax: +86-25-8082-5498.

Academic Editor: Marc Rosen

Received: 21 May 2015 / Accepted: 4 August 2015 / Published: 14 August 2015

Abstract: In room–corridor building geometry, the corridor smoke temperature is of great importance to fire protection engineering as indoor fires occur. Theoretical analysis and a set of reduced-scale model experiments were performed, and a virtual fire model was proposed, to investigate the correlations between the maximum smoke temperature in corridors and the smoke temperature in rooms. The results show that the dimensionless virtual fire heat release rate (HRR) is characterized by quadratic-polynomial of the dimensionless smoke temperature in fire rooms. The dimensionless distance from a virtual fire source to the corridor ceiling varies linearly with the dimensionless smoke temperature in a room. Results of multiple regression indicate that, at the impingement area of virtual fire, the dimensionless maximum smoke temperature in corridors is only related to the dimensionless virtual fire HRR; in the non-impingement area of a virtual fire, the dimensionless maximum smoke temperature in corridors is a function of the dimensionless virtual fire HRR and dimensionless longitude distance. The viscosity and conduction exhibit an insignificant impact on the maximum temperature in the corridor. Through replacing the parameters of virtual fire with the dimensionless smoke temperature in fire rooms, the correlations between dimensionless maximum temperature in corridors and the dimensionless smoke temperature in fire rooms were proposed.

Keywords: room-corridor fire; maximum smoke temperature; virtual fire; dimension analysis

1. Introduction

The hot smoke of building fires is a critical problem for fire protection engineering. The safety of the occupants and firefighters in the contaminated area is severely affected by the fire-induced hot smoke. Actually, toxic smoke has led to about 85% of deaths in building fires [1]. During fires, the hot smoke can directly burn people, even resulting in death [2]. Moreover, the hot smoke and flame can reduce the strength of the steel bars in concrete, thus directly affecting the structure of the building and eventually leading to building collapse [3]. Besides, the detectors and sprinklers are activated by the maximum smoke temperature beneath the building ceiling. Room and corridor are the basic compositions of a building, and room–corridor is a common geometry in some buildings. Under some conditions, when the fire occurs in a room, people escape through the corridor. Therefore, it is very important to study the maximum smoke temperature under the corridor ceiling to attain the safety level of the building. Advanced computer modeling software, which can predict smoke spread and compartment temperatures, has been developed during the last decade. However, simple correlations to obtain a first estimate of smoke temperatures are still highly desirable. McCaffrey *et al.* [4] developed classic MQH correlation based on simple conservation of energy expression, through over 100 experiments, which could simply and rapidly estimate the average hot smoke temperature in compartment fires. An alternate model was proposed by Sharma *et al.* [5] for compartment fire temperature based on an energy balance and an empirical mass flow rate formula, which alleviated the two major limitations of the MQH correlation. Chen *et al.* [6] investigated the correlations of peak hot gas temperature with first and second order gradients during fire growth, and the results of one full-scale test were in good agreement with the critical conditions indicated by the small-scale tests. Quintiere *et al.* [7] investigated the thermal and flow environment within a corridor subjected to a room fire, and achieved good correlating results between the model and full-scale experiments. Alpert *et al.* [8] provided simple correlation equations to predict the maximum temperature and velocity at a given position, based on a generalized theory and experimental data. Kurioka *et al.* [9] proposed a model to predict the maximum smoke temperature under the tunnel ceiling based on model-scale experiments. Hu *et al.* [10–12] conducted a series of full-scale experiments to investigate the smoke temperature distribution, velocity, and maximum temperature along the corridor. Ji *et al.* [13–16] conducted reduced-scale experiments, and obtained a simplified calculation to predict the maximum temperature under the ceiling, and investigated the transverse smoke temperature distribution in road tunnel fires. Moreover, they also analyzed the influence of different transverse fire locations and sidewall restriction on the maximum ceiling smoke temperature. Johansson and Hees [17] developed a correlation based on the results from computer simulations that predicted gas temperatures in a room adjacent to a room involved in a pre-flashover fire. The external validity was studied by comparing the correlation results with full-scale test data. Gao *et al.* [18] introduced a modified concept of virtual origin to calculate the maximum ceiling gas temperature in the presence of a hot upper layer beneath

ceiling. They translated the confined plume in the hot upper layer into the free plume in the open space by the modified virtual fire.

Most of the abovementioned studies focused on the smoke diffusion and temperature due to separate compartment fires or tunnel/corridor fires. However, actually, lots of fires can be classified as room–corridor fires, *i.e.*, the fire occurs in a room and the smoke propagates to the corridor through the door. The smoke temperature in the corridor could severely affect the safety of the occupants. Some studies investigated the smoke temperature in rooms and corridors, respectively. In the room–corridor geometry fire [7,19], however, little attention has been paid to the correlations between the corridor temperature and the smoke parameters in the fire room. Therefore, in this study, a set of reduced-scale room-corridor experiments were performed to develop the empirical correlations between the maximum smoke temperature under the corridor ceiling and the measured smoke temperature in a fire room.

2. Theoretical Analysis

2.1. Mass Doorflow Rate

Thomas [20] provided a brief review of the modeling of fire growth in compartments and explained the main lines of development and discussed some of the questions raised by each type of modeling. Rockett [21] studied the flow of gases in and out through a vent in an enclosure, analyzed pressure profiles and vent flows, and built a zone model to compute mass flow rate through the door. A two-zone model with uniform properties was used as depicted in Figure 1, which demonstrates that mixing occurs in the interface due to the plunging of the cold door air jet through part of the upper hot layer. The two-zone model represents the enclosure as consisting of two distinct gas zones: A lower volume of ambient temperature, as is the temperature outside of the enclosure; and an upper volume with uniformly distributed hot gas. Rockett derived the equations to calculate the mass flow rate in and out of the door based on the pressure profile, as follows:

$$\dot{m}_{out} = \frac{2}{3} C_d w \rho_r \sqrt{\frac{2(\rho_\infty - \rho_r)g}{\rho_r}} (H_O - H_N)^{3/2} \quad (1)$$

$$\dot{m}_{in} = \frac{2}{3} C_d w \rho_\infty \sqrt{\frac{2(\rho_\infty - \rho_r)g}{\rho_r}} (H_N - H_D)^{1/2} (H_N + \frac{1}{2} H_D) \quad (2)$$

In the abovementioned equations, the smoke layer height H_D could be visually recorded. The height of neutral plane H_N could not be determined from experimental data. However, by equating Equations (1) and (2) with the assumption that the fuel loss rate is negligible (mass in-flow equals mass out-flow under this assumption), H_N could be solved. Finally, H_N was substituted to Equation (1), and the quantitative estimation of the mass flow rates was made.

2.2. Virtual Fire

Considering a simple type of fire plume, which is also called the ideal plume or the point-source plume, Heskestad [22] established the fundamental equations for buoyancy, momentum, and continuity; and thus obtained analytical solutions for the temperature and mass flow of the hot smoke

gases in this simplified plume. The corresponding equations for the plume mass flow and plume temperature increase could be written as follows:

$$\dot{m}_p = 0.2\ (\frac{\rho_\infty^2 g}{c_p T_\infty})^{1/3}(\dot{Q}_v)^{1/3} \bullet z^{5/3} \tag{3}$$

$$\Delta T_g = 5.0(\frac{T_\infty}{c_p^2 \rho_\infty^2 g})^{1/3} \dot{Q}_v^{2/3} \bullet z^{-5/3} \tag{4}$$

where $\dot{Q}_v$ is virtual fire HRR, (kW), and z is the distance from door soffit to the virtual fire source, (m). In general, $\dot{Q}_v$ and z are treated as known numbers to calculate $\dot{m}_p$ and ΔT_g. However, in contrast, if set $\dot{m}_p$ and ΔT_g as known numbers, $\dot{Q}_v$ and z can be obtained by combining Equations (3) and (4). Thus, to obtain a relationship between corridor smoke temperature and smoke parameters in room, as shown in Figure 1, smoke mass flow rate and temperature were assumed to be constant when it moved out from the vertical door plane to the horizontal door soffit plane ($\dot{m}_{out} = \dot{m}_p$, $\Delta T_g = \Delta T_r$). In other words, ambient cold gas was not entrained by the smoke gas during this process. Moreover, the smoke at the horizontal plane of door soffit was considered as the result of a virtual point-source fire flush with the wall at the centerline of the door. Therefore, the virtual fire would be the bridge to connect corridor temperature to the parameters in the fire room.

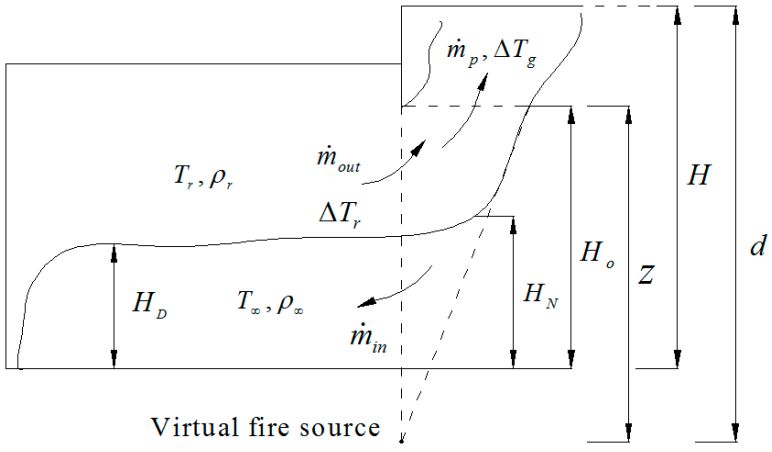

Figure 1. Schematic representation of the two-zone model.

Zukoski [23] studied the fire sources placed near or flushed with walls and corners which restricted the entrainment of the fire plume. For the plume attached to the wall and developed as a half plume with properties approximating those for a full burner with twice the energy release rate and half of the plume mass flow, the wall fire mass flow rate could be written as follows:

$$\dot{m}_p = 0.5 f(2\dot{Q}_v) \tag{5}$$

Substituting Equation (5) into Equations (3) yields:

$$\dot{m}_p = 0.1\ (\frac{2\rho_\infty^2 g}{c_p T_\infty})^{1/3} \dot{Q}_v^{1/3} \bullet z^{5/3} \tag{6}$$

Substituting Equation (6) into the equation $\dot{Q}_v = c_p \dot{m}_p \Delta T_g$ yields:

$$\Delta T_g = 10(\frac{T_\infty}{2c_p^2\rho_\infty^2 g})^{1/3}\dot{Q}_v^{2/3}\bullet z^{-5/3} \tag{7}$$

where $\dot{m}_p$ and ΔT_g are treated as known numbers and $\dot{m}_{out} = \dot{m}_p$, $\Delta T_g = \Delta T_r$, based on Equations (1), (6) and (7), dimensionless temperature is defined as $y = T_r/T_\infty$, $\dot{Q}_v$ and z could be expressed as:

$$\dot{Q}_v = 235.33C_d w c_p(1-\frac{1}{y})\sqrt{2g(y-1)}(H_O - H_N)^{3/2} \tag{8}$$

$$z = 3.39(C_d w)^{2/5}(H_O - H_N)^{3/5}y^{-2/5} \tag{9}$$

The standard values for the right hand side of Equations (8) and (9) are: (a) specific heat of air (c_p) = 1.006 kJ·kg^{-1}·K^{-1}; (b) gravitational acceleration (g) = 9.795 m·s^{-2}. In general, the value of C_d = 0.6−0.7 is valid for wide range of fire safety engineering applications. Steckler *et al.* [24] reported that door flow could be regarded as inviscid and buoyancy driven owing to temperature differences with an "orifice" vent coefficient of 0.7 ± 0.03. Therefore, C_d = 0.7 was used as the optimum value in this study. Thus, Equations (8) and (9) could be rewritten as:

$$\dot{Q}_v = 733.484w(y-1)^{3/2}(H_O - H_N)^{3/2}y^{-1} \tag{10}$$

$$z = 2.939w^{2/5}(H_O - H_N)^{3/5}y^{-2/5} \tag{11}$$

2.3. Dimensional Analysis

The virtual point-source fire model was established and it was assumed that the virtual corridor fire had the same effect from the room to the corridor. Thus, the most important role of virtual fire was to connect the gas parameters between the room and corridor. Actually, the process of setting virtual fire was based on some assumptions, and it should be performed with care through evaluations of its assumptions which were somewhat different from the reality. However, the smoke layer temperature in the room will replace the parameters ($\dot{Q}_v$, z) standing for virtual fire in the last Equation (40). Therefore, the virtual fire acted like a "bridge" to connect the smoke temperature in the corridor and smoke temperature in the room. Thomas [25] discussed certain examples critically and commented on the analysis of experimental data in the context of dimensional analysis. Dimensional analysis was performed to acquire the law of maximum smoke temperature along the corridor. Extensive research efforts have been devoted to the use of dimensionless parameters to analyze the fire model and process in order to simplify the relationship among the physical parameters. Sharma *et al.* [5] made use of dimensional parameters to study the compartment fire temperature. Lei Wang [26] took advantage of dimensional analysis to analyze the compartment doorway flows. In this study, Buckingham's theorem [27] was used to obtain the dimensionless parameters affecting the maximum temperature along the corridor. The following hypothesis was made:

(a) The role of virtual point-source fire was equivalent to the effect of fire from room to corridor;
(b) There was no radiation loss for virtual point-source fire, all the virtual fire energy was released through convection;

Based on the abovementioned analysis and assumptions, and according to Buckingham's theorem [27], the following dimensionless parameters were obtained:

Temperature:

$$\theta^* = \frac{\theta}{T_\infty} \tag{12}$$

where $\theta = T_{b,max} - T_\infty$

Distance:

$$r^* = \frac{r}{d} \tag{13}$$

where d is the distance from virtual fire source to corridor ceiling, $d = z + (H - H_o)$

Firepower:

$$Q_v^* = \frac{\dot{Q}_v}{c_p T_\infty \rho_\infty \sqrt{gd}\, d^2} \tag{14}$$

Conduction term:

$$h_v^* = \frac{h_v}{\rho_\infty c_p \sqrt{gd}} \tag{15}$$

where h_v is the effective conduction heat transfer coefficient. Tanaka and Yamada [28] obtained the empirical correlations between dimensionless effective conduction coefficient and dimensionless fire HRR as follows:

$$h_v^* = \frac{h_v}{\rho_\infty c_p \sqrt{gd}} = \begin{cases} 2\times10^{-3}, \dot{Q}_v^* \le 4\times10^{-3} \\ 0.08\dot{Q}_v^{*2/3}, \dot{Q}_v^* > 4\times10^{-3} \end{cases} \tag{16}$$

Reynolds number:

$$R_v^* = \frac{\rho_\infty \sqrt{g} d^{3/2}}{\mu} \tag{17}$$

where μ is the dynamic viscosity, and the relationship between viscosity and air temperature could be written as [29]:

$$\mu = \mu_{20} \exp\left(\frac{\mathrm{d}(\ln \mu)}{\mathrm{d}T} \times [T(\mathrm{K}) - 20]\right) \tag{18}$$

$\mu_{20} = 1.82 \times 10^{-5}$, at the standard atmospheric pressure, and $\mathrm{d}(\ln\mu)/\mathrm{d}T = 2.56 \times 10^3$.

To explore the maximum temperature in the nearby corridor ceiling, four dimensionless parameters were considered as obeying the following relationship:

$$\theta^* = f(r^*, Q_v^*, H_v^*, R_v^*) \tag{19}$$

In general, when dealing with the experimental data, it was assumed that left hand side of Equation (19) changed as some power of r^*, $\dot{Q}_v^*$, H_{*v} and R_{*v}, thus, Equation (19) could be rewritten as:

$$\theta^* = n(r^*)^a (Q_v^*)^b (H_v^*)^c (R_v^*)^d \tag{20}$$

If smoke was assumed to be ideal inviscid gas, R_{*v} could be removed and Equation (20) could be modified as:

$$\theta^* = n(r^*)^a (Q_v^*)^b (H_v^*)^c \quad (21)$$

The parameters in Equations (20) and (21) could be obtained from experimental data, and the Equations (20) and (21) could be achieved through multiple regression of the data obtained from the experiment.

3. Experiments

The experiments were performed in a reduced-scale room-corridor structure model, Figure 2a shows the sketch of the experimental model. A scale ratio of 1:4 was applied to perform the reduced-scale experiments. The size of the room and corridor is illustrated in Figure 2b, the corridor is 16 m long, the width and height of corridor could be changed under different cases. The end face of the corridor near room is sealed and the other end face is kept open. The door height is 0.5 m and width is 0.2 m. Room walls were made of the tempered glass, which could resist the high temperature of fire. Polycarbonate sheet was used as corridor wall to observe the progress of the experiment.

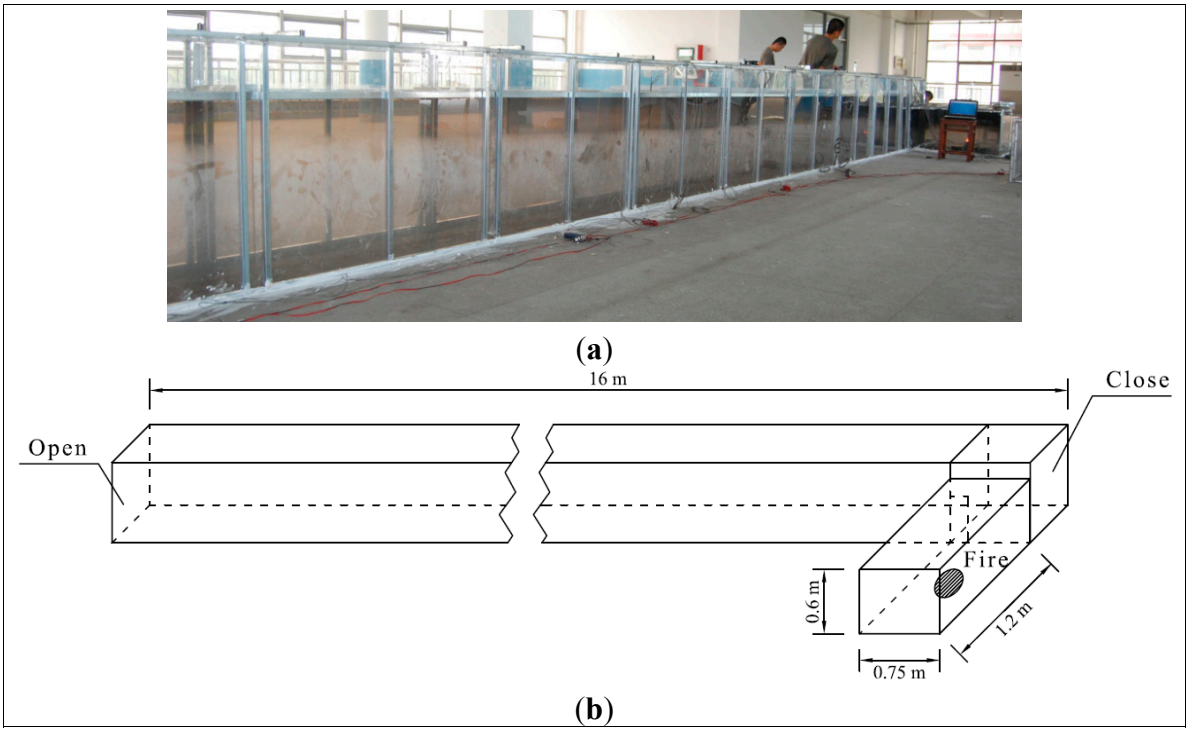

Figure 2. (**a**) Photo of experimental room-corridor model; and (**b**) Schematic representation of the experimental apparatus.

The physical scale model was prepared by using the Froude modeling. The scaling laws, dimensional relationships of the physical variables between the reduced-scale and full-scale models could be obtained through the Froude modeling. Equations (22) and (23) are used to scale the temperature (T) and HRR (Q), the model size is represented by L, the subscripts "m" and "f" denote the model and full-scale structures, respectively.

$$T_m = T_f \tag{22}$$

$$\frac{\dot{Q}_m}{\dot{Q}_f} = \left(\frac{L_m}{L_f}\right)^{5/2} \tag{23}$$

Heptane pool fire was used to simulate the fire source, which was located in the center of the room. The HRRs were computed using the following equation:

$$\dot{Q} = \alpha m_f \Delta H \tag{24}$$

where α is the combustion efficiency, m_f is the mass loss rate of fire, and ΔH is the heat of combustion. Heptane was used as fuel of pool fire, and α is the efficiency of combustion which is about 0.6–0.8 [30]. Babrauskas [31] reported that for the fuel yielding a low amount of soot, the recommended value of α is 0.8 and the ΔH of heptane is 44.6 kJ·g^{-1}. m_f was measured by the electronic balance connected to the computer, and the precision of electronic balance was 0.01 g. A mass data acquisition system was used for mass measurements with 5 s sampling intervals.

Three kinds of circle-shaped pools were used with diameter 0.1 m, 0.141 m, 0.2 m, respectively; moreover, at the same time, the height and width of the corridor were changed, and the corresponding values are listed in Table 1. Ten experiments with different cases were performed, and each test was carried out twice. Based on the data obtained from the experiment, HRR of the pool fire in the room could be acquired by using Equation (24), the virtual fire HRR and the distance between virtual fire and corridor ceiling could be calculated through Equations (10) and (11), and based on the development of virtual fire HRR changing with time, we could obtain the maximum virtual fire HRR. The dimensionless virtual fire HRR could be obtained through dimensional analysis as per Equation (14). Table 1 lists the fire and corridor parameters of all the experiments; moreover, the virtual fire HRR and the dimensionless virtual fire HRR are also listed in Table 1.

Table 1. Model experiment parameters and HRR (heat release rate).

Case No.	Pool Diameter (cm)	Fuel Volume (mL)	Corridor Height (cm)	Corridor Width (cm)	Q_{max} (kW)	$Q_{v,max}$ (kW)	$Q_{v,max}$ × 10^{-3}
1	10	100	75	50	9.76	1.38	1.79
2	14.1	200	75	50	29.7	2.97	4.2
3	20	300	75	50	63.11	3.66	5.59
4	10	100	75	40	9.54	1.31	1.7
5	14.1	200	75	40	29.46	2.96	4.18
6	10	100	75	60	12.18	1.5	1.97
7	14.1	200	75	60	31.07	3.07	4.37
8	10	100	60	50	11.99	1.94	2.56
9	14.1	200	60	50	31.56	3.49	5.03
10	20	300	60	50	65.58	4.73	7.27

All experiments were started at ambient temperatures of about 34–37 °C. The temperature distributions along the corridor were measured by thermocouples. K-type shielded thermocouples were used to measure the temperature, and the measuring range was 0–1300 °C. According to reference [32], the measurement error of the thermocouple was less than 1 °C (0–120 °C), and the error would be within

7% when temperature is less than 500 K. All the thermocouples were calibrated in boiling water prior to their use to make sure the accuracy of thermocouples is less than 1 °C. The radiation correction is difficult to perform precisely, because determination of effective surrounding temperatures is difficult in different environments. However, the maximum radiation error could still be estimated from the results of previous theoretical work [33], whereby the radiation error is less than 6% for the typical smoke temperature of this work. Eight sets of thermocouples in total are mounted in the model, as shown in Figure 3, three sets in the fire room and five sets in the corridor, respectively. Each set consists of eight thermocouples placed vertically in the room, and the distances between the ceiling and thermocouples are 1, 9, 17, 25, 33, 41, 49 and 57 cm, respectively. Besides, for the Cases 1–7, six thermocouples in each set are placed vertically in the corridor, and the distances between thermocouples and ceiling are 1, 15, 29, 43, 57 and 71 cm, respectively. Cases 8–10 consist of five thermocouples in each set placed vertically in the corridor, and the distances between thermocouples and the ceiling are 1, 15, 29, 43 and 57 cm, respectively. Experiments made use of the I/O module transmitting the thermocouples temperature to the computer, a data acquisition system was used to record and store the temperature measurements, and the sampling interval was 5 s.

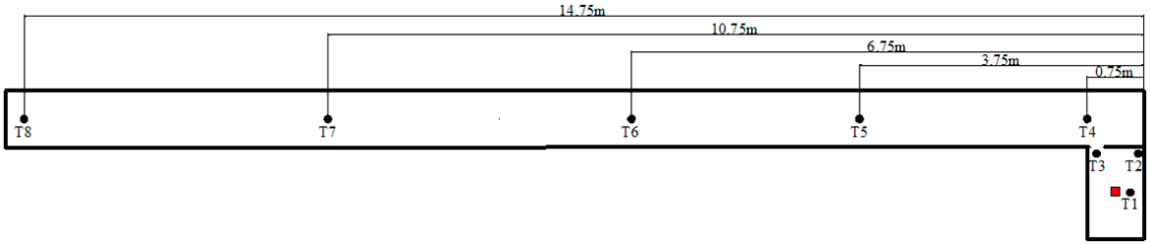

Figure 3. Schematic representation of the thermocouples mounted in the model.

4. Results and Discussion

4.1. Virtual Fire HRR and the Distance from Virtual Fire Source to Corridor Ceiling

Virtual fire HRR and the distance from the virtual fire source to the corridor ceiling are typical parameters to describe virtual fire. Investigating the virtual fire HRR and the distance from the virtual fire source to the corridor was the first step in this study. The virtual fire HRR and the distance from the virtual fire source to the corridor ceiling could be obtained by Equations (10) and (11), respectively. Figure 4 shows that the virtual fire HRR increases to the maximum in the early experimental stage and then declines at a later stage, which is similar to pool fire HRR *vs.* time in the room. The virtual fire HRR was calculated based on the mass flow rate of smoke from room to corridor. When the pool fire fuel was burned out completely, the smoke temperature in the room was still high and smoke would continue to flow out into the corridor. Therefore, when the pool fire was burned out, the virtual fire did not decline to zero. When further experiments were performed at the same pool fire and corridor height, the change in virtual fire HRR *vs.* time did not show any significant differences, although width of the corridor was different. However, under similar conditions of pool fire and corridor width, the lower corridor height resulted in a more rapid increase in the virtual fire HRR

at the early stage and faster decline at the later stage. Moreover, the virtual fire peak HRR was greater with the lower corridor height.

The corridor dimensionless ratio of width to height was defined as $W^* = W/H$. Figure 5 reveals the relationship between the virtual fire peak HRR and the dimensionless width to height ratio W^*. The maximum virtual fire HRR increases with an increase in W^*. The increase in W^* due to a change in the width leads to insignificant change in the maximum HRR; however, the increase in W^* due to a change in height results in maximum visible change in the HRR. Thus, the abovementioned analysis indicated that, the corridor height had great impact on the maximum dimensionless virtual fire HRR, however, the corridor width hardly influenced the maximum dimensionless virtual fire HRR.

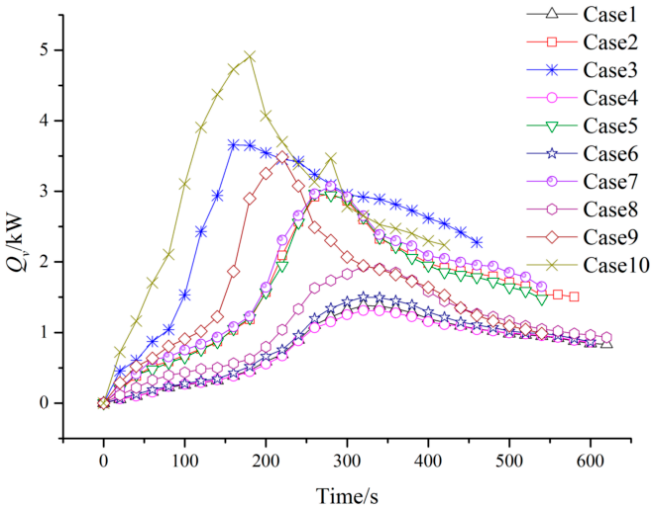

Figure 4. Virtual fire HRR under all cases.

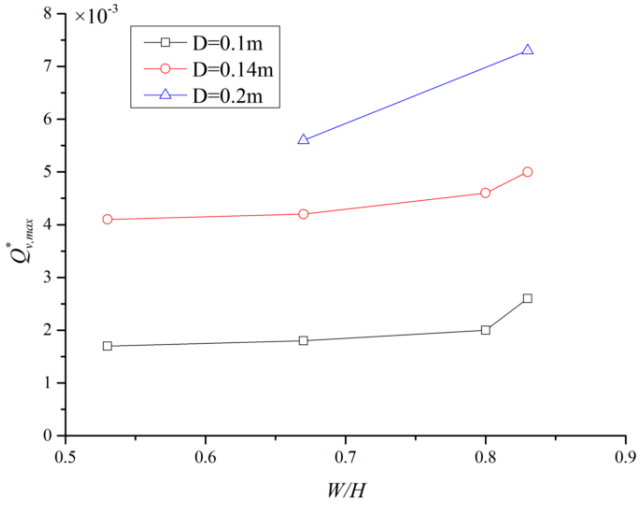

Figure 5. Change in the maximum virtual fire HRR against W^*.

Figure 6 shows that in all the experiments, the distance from virtual fire source to corridor ceiling decays as the virtual fire HRR increases at early stage. When the virtual fire HRR reaches the peak, the distance from the virtual fire source to the ceiling becomes minimum, and then increases a little with the decay of virtual fire HRR. The larger the maximum virtual fire HRR, the smaller is the minimum distance from virtual fire source to ceiling.

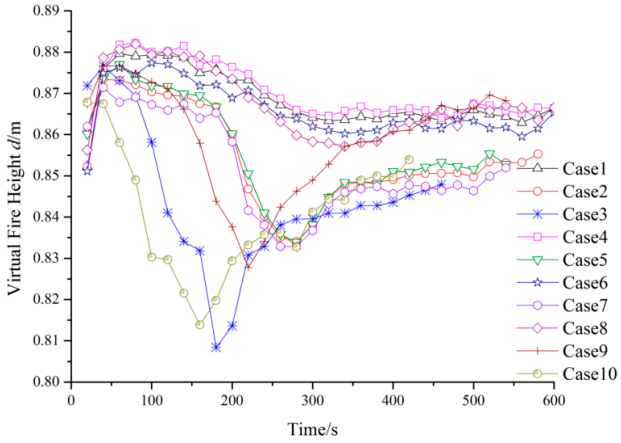

Figure 6. Distance from virtual fire source to corridor ceiling in all cases.

4.2. Correlations between the Virtual Fire and Smoke Temperature in Fire Room

The virtual fire acted as a bridge between the real fire in the room and the maximum temperature in the corridor, thus we need to obtain the correlations between the virtual fire and real fire in room. Indeed, the correlations between the virtual fire and the maximum temperature in the corridor was also required. Alpert [34] concluded that the maximum smoke temperature occurred at the position of $0.01H$–$0.02H$ below the ceiling. The positions of the top thermocouples on the sets of thermocouples in corridor were in the range concluded by Alpert. Some physical parameters were obtained to replace the virtual fire HRR and position, the correlations between the real fire in room and maximum temperature in corridor could be achieved.

The dimensionless virtual fire source position d^* was defined as follows:

$$d^* = d / H \tag{25}$$

The distance from virtual fire source to corridor ceiling and HRR were the characterized parameters representing the virtual fire, non-dimensionalization of the virtual fire HRR and distance was required in all the cases by Equations (14) and (25), respectively. Figures 7 and 8 show the plots of the dimensionless virtual fire HRR and dimensionless virtual fire distance against the dimensionless smoke temperature in the fire room, respectively. Figure 7 shows that dimensionless virtual fire HRR Q_v^* increases/declines as dimensionless smoke temperature y increases/decreases. The correlation, regardless of the increase or decrease in the dimensionless Q_v^*, could be fitted as:

$$Q_v^* = a_1 y^2 + b_1 y + c_1 \tag{26}$$

where a_1, b_1 and c_1 are constants, and the value of a_1, b_1 and c_1 are 0.0124, −0.0178, 0.0052, respectively, with the adjusted coefficient of determination [35] being greater than 0.99:

$$Q_v^* = 0.0124 y^2 - 0.0178 y + 0.0052 \tag{27}$$

Figure 8 shows the linear relationship between the dimensionless distance from virtual fire source to corridor ceiling and dimensionless smoke temperature in room, and it could be fitted as:

$$d^* = b_2 y + c_2 \tag{28}$$

where b_2 and c_2 are constants.

The experimental results indicated that corridor width had little impact on the relationship between the position of the virtual fire source and dimensionless smoke temperature in fire room, as long as the height of the corridor was kept constant. Without considering other parameters, the correlation between d^* and y could be fitted as one line in different corridor height cases. Therefore, corridor height was the primary parameter influencing the position of the virtual fire source and dimensionless smoke temperature in the fire room. The experimental results were well fitted as follows, with the adjusted coefficient of determination being greater than 0.90:

$$d^* = -0.168y + 1.348 \text{ , } H = 0.75 \text{ m} \tag{29}$$

$$d^* = -0.221y + 1.704 \text{ , } H = 0.6 \text{ m} \tag{30}$$

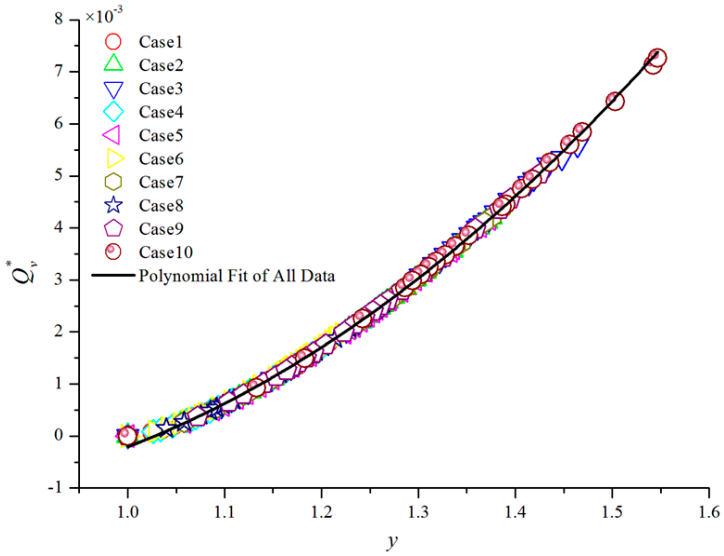

Figure 7. Dimensionless virtual fire HRR as a function of dimensionless average smoke temperature in the room.

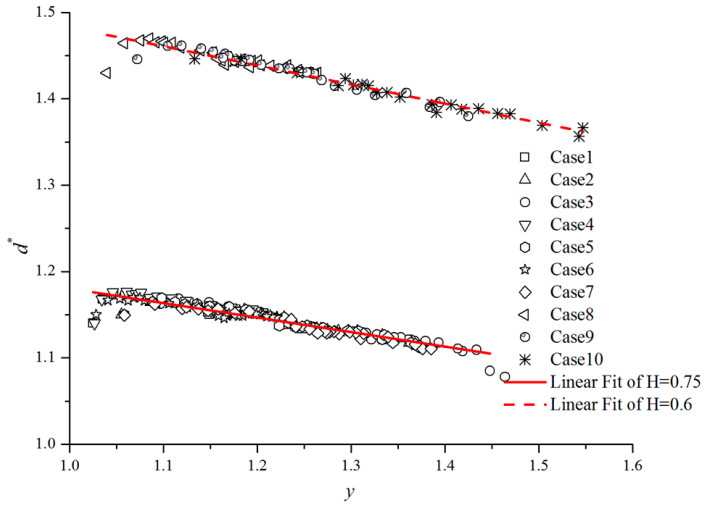

Figure 8. Dimensionless distance from virtual fire source to corridor ceiling as a function of dimensionless average smoke temperature in room.

4.3. The Correlations between Virtual Fire and Real Pool Fire in Room

McCaffrey *et al.* [4] presented the classic MQH correlation based on eight sets of data comprising over 100 experiments, the empirical relates Q^* and y, and estimates the "average temperature" in the upper part, as follows:

MQH correlation:

$$y-1=1.63\frac{Q^{*2/3}}{h^{*1/3}};y<3 \tag{31}$$

where $Q^*=\frac{\dot{Q}}{c_pT_\infty\rho_\infty\sqrt{gD}D^2}$ is the dimensionless pool fire HRR in room; D is pool diameter; and dimensionless conduction term: $h^*=\frac{hA}{\rho_\infty c_pA_o\sqrt{gH_o}}$, h is the effective conduction heat transfer coefficient, A is the area of the walls in the fire room, and A_o is the area of the door.

In terms of the correlation between average smoke temperature and real pool fire established by using MQH equation, and based on the relationship between virtual fire and average smoke temperature in the room, Equation (31) could be substituted in Equations (26) and (28), respectively, thus the correlations between virtual fire Q_v^*, d^*, and real pool fire HRR were obtained.

4.4. Maximum Temperature in the Corridor

The correlations between virtual fire and smoke temperature in fire room were obtained above. We were then required to investigate the correlations between the maximum temperature in the corridor and the virtual fire. Based on these two sets of correlations, the correlations between the maximum temperature in corridor and the smoke temperature in fire room could be obtained through the "bridge" of the virtual fire. Firstly, we need to investigate the maximum temperature decay law in corridor, and the virtual fire application in classic Alpert's correlations [8]. The dimensionless maximum smoke temperature increases with the dimensionless distance as shown in Figure 9. The experimental results and fitting data indicated that the increase in the maximum smoke temperature seemed to decay exponentially with increasing distance, which could be fitted as follows:

$$\theta^*=b_3e^{(-(r/d)/a_3)}+c_3 \tag{32}$$

where a_3, b_3 and c_3 are constants.

Figure 9 shows that corridor width has negligible influence on the maximum temperature under ceiling. The results were similar to that obtained from the study of Ying and Haukur [36]. They demonstrated that the tunnel maximum temperature beneath the ceiling was independent of tunnel width. Besides, the maximum temperature increased notably with the reduction in the height of the ceiling, provided the other parameters were kept constant. The influence of height decreases with increasing distance, and the maximum temperature inclined to be uniform at the distal of the corridor in all experimental cases.

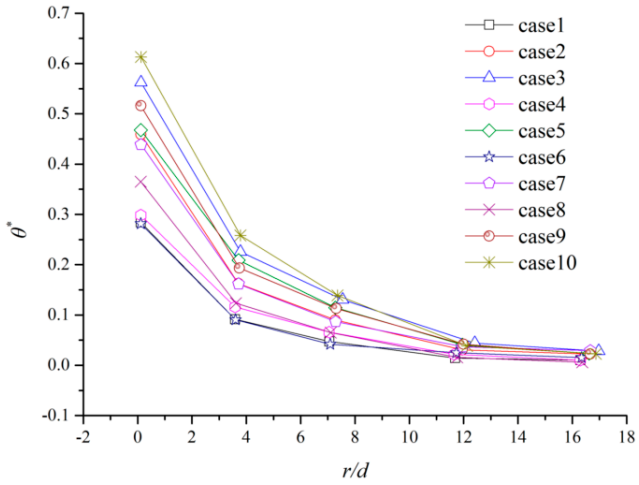

Figure 9. Increase in maximum corridor temperature in all cases.

Alpert [8] has developed easy to use correlations to quantify the maximum gas temperature through smoke plume experiments. These correlations are extensively used in the hazard analysis calculations. Alpert's correlations for maximum ceiling jet temperatures are as follows:

$$T_{b,\max} - T_{\infty} = \begin{cases} \dfrac{16.9Q^{2/3}}{d^{5/3}}, & r \le 0.18d \\ \dfrac{5.38}{d}\left(\dfrac{Q}{r}\right)^{2/3}, & r > 0.18d \end{cases} \tag{33}$$

Virtual fire HRR was substituted in the Alpert's equation to predict the maximum temperature increase in the corridor. The maximum temperature increase measured in experiments and predicted by the Alpert's equation are plotted in Figure 10, when $r \le 0.18d$. Figure 10 shows insignificant difference between the experimental results and the Alpert's model prediction in all the cases. The errors between the experimental results and Alpert's equation prediction are listed in Table 2. In seven cases, the error was within 10%, and only in three cases the error was about 13%. The average error was 6.1% obtained through computing. Thus, the Alpert's correlation using virtual fire HRR could be used to predict the maximum temperature in the impingement area.

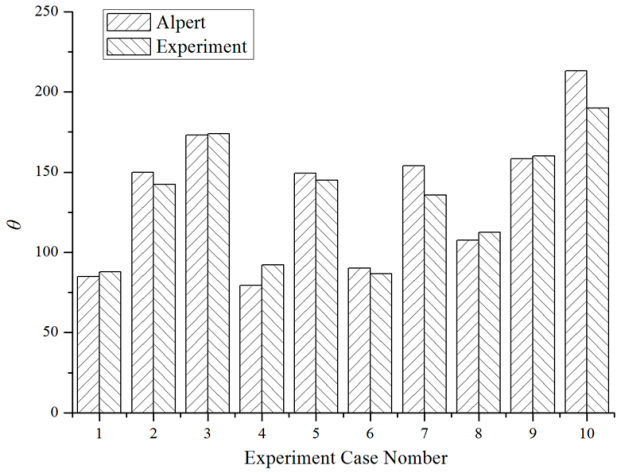

Figure 10. Comparison of the maximum temperature increase in the impingement region.

Table 2. Error between measured and calculated maximum temperature increase.

Case NO.	1	2	3	4	5	6	7	8	9	10
Experiment/K	87.9	142.4	173.9	92.2	144.9	86.8	135.6	112.5	160	190
Alpert/K	85	149.9	173.1	79.3	149.3	90.2	153.9	107.7	158.3	213.2
Error/%	3.33	5.28	0.43	13.97	3.03	3.89	13.46	4.3	1.07	12.19

In the region with $r > 0.18d$, the correlation between the experimental results and Alpert's equation prediction is hypothetically fitted as shown in Figure 11. The maximum temperature increase measured by the experiments was different from the Alpert's equation prediction. The experimental results were higher than the Alpert's equation prediction, because smoke movement was confined by the walls; however, they could be fitted linearly as follows:

$$\theta = b_4 \theta_{Alpert} + c_4 \tag{34}$$

where b_4 and c_4 are constants.

The experimental results are well fitted as follows, with the adjusted coefficient of determination as 0.95:

$$\theta = 3.365\theta_{Alpert} - 12.564 \tag{35}$$

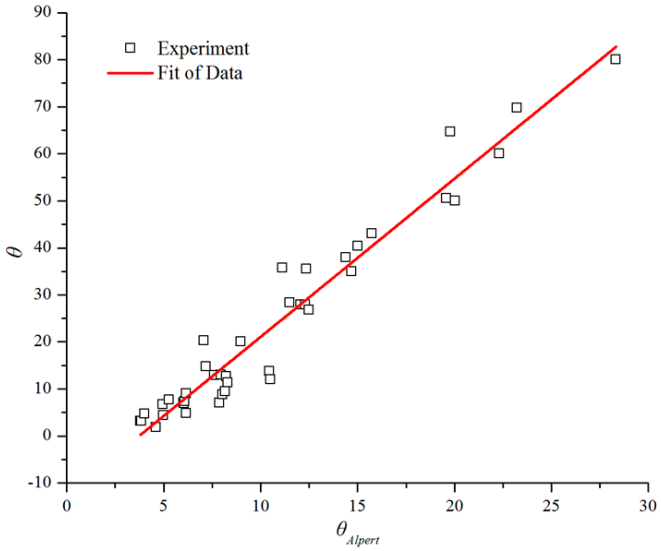

Figure 11. Comparison of maximum temperature increase in the non-impingement region.

4.5. Model for the Prediction of Maximum Temperature in Corridor

Ten experimental cases were performed to investigate the model to predict the maximum temperature in the corridor. Based on the investigation above, dimensional analysis was performed to obtain the dimensionless parameters, namely, θ*, r*, Q_v^*, H_v^* and R_v^*, affecting the maximum temperature in the corridor. Through the multiple regression of the dimensionless parameters, θ*, r*, Q_v^*, H_v^* and R_v^* and based on the experimental data, Equation (20) was followed and the values of a, b, c, d and n were −0.5305, 0.8517, 0.0681, −0.2718 and 6.4538, respectively.

Investigation of multiple linear regression indicated that some dimensionless parameters almost had no influence on the results, therefore, they should be analyzed and acquired. They kept the key dimensionless parameters to establish the model. θ* is defined as follows: $\theta^* = n \times (r^*)^a \times (Q_v^*)^b \times (H_v^*)^c \times (R_v^*)^d = n \times (X_1)^a \times (X_2)^b \times (X_3)^c \times (X_4)^d$. When regression analysis was performed on different parameters, the values of root mean square error/standard error (RMSE) and decision coefficient (*R*-square) were obtained (Table 3). The comparison of the results indicated that the variable group X_1, X_2; X_1, X_2, X_3; X_1, X_2, X_4; X_1, X_2, X_3, X_4 had the same decision coefficient. However, the variable group X_1, X_2 had the minimum value of RMSE. Therefore, r^* and Q_v^* were the key parameters influencing the maximum temperature increase in the corridor. Besides, the same result was obtained by performing the "stepwise" regression through MATLAB as shown in Figure 12.

Table 3. Standard error and decision coefficient based on different parameters.

	X_1, X_2	X_1, X_3	X_1, X_4	X_2, X_3	X_2, X_4	X_3, X_4	X_1, X_2, X_3	X_1, X_2, X_4	X_2, X_3, X_4	X_1, X_2, X_3, X_4
***R*-square**	0.83	0.78	0.8	0.2	0.7	0.71	0.83	0.83	0.7	0.83
RMSE	0.51	0.58	0.56	1.12	0.68	0.68	0.52	0.52	0.68	0.52

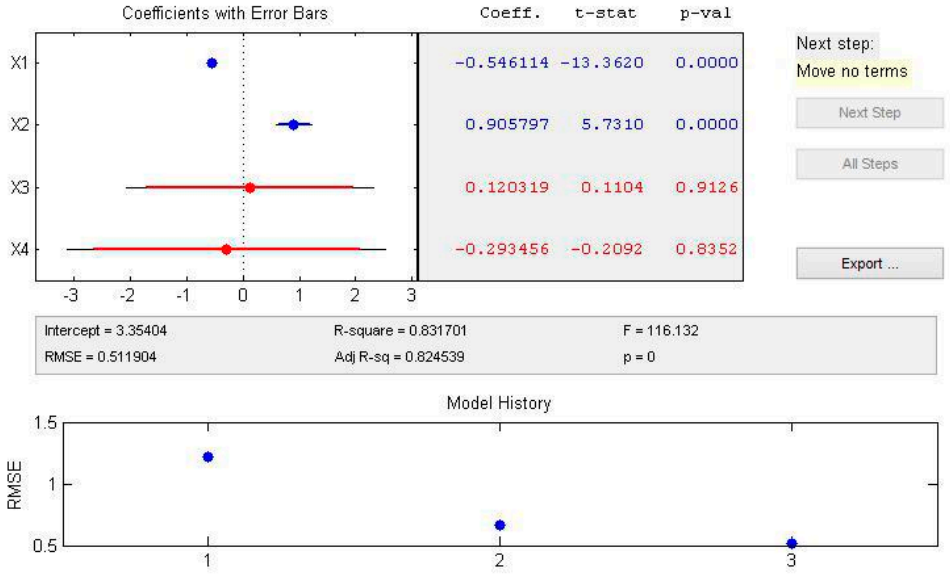

Figure 12. Stepwise regression results of MATLAB.

The abovementioned analysis indicated that, the dimensionless viscosity and heat conduction exhibited insignificant impact on the maximum temperature increase; however, the dimensionless distance and virtual fire HRR were the key parameters affecting the maximum temperature increase. Subsequently, the correlation between θ* and r^*, Q_v^* could be expressed as follows:

$$\theta^* = n(r^*)^a (Q_v^*)^b \tag{36}$$

Therefore, by the multiple regression of the experimental results, Equation (36) could be rewritten as Equation (37), with the adjusted coefficient of determination as 0.82.

$$\theta^* = 28.617(r^*)^{-0.5462} (Q_v^*)^{0.9058} \tag{37}$$

The experimental results and the analysis of the regression prediction model are plotted in Figure 13. Figure 13 clearly shows some difference between the experimental results and regression model, especially, at the right side of the X-axis, although the adjusted coefficient of determination is 0.82.

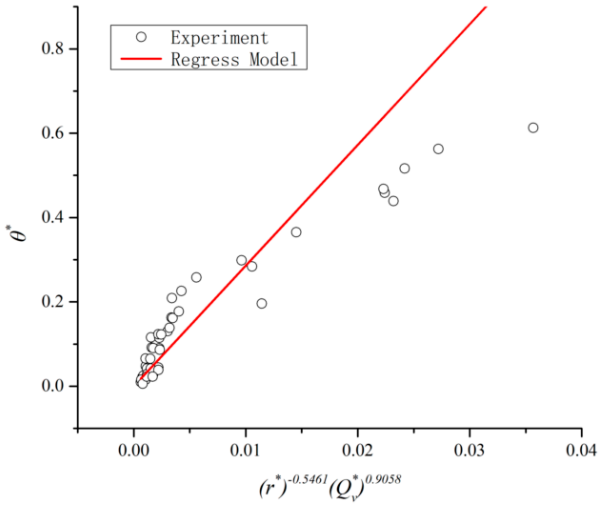

Figure 13. Measured and regression model used for the estimation of the dimensionless maximum temperature increase.

Alpert [8] defined $r = 0.18\ d$ as the boundary of fire impingement and non-impingement areas, the data showed at $0 < (r^*)^{-0.5461} \times (Q_v^*)^{0.9058} < 0.01$ by Figure 13 correspond to the area of $r < 0.18d$ (virtual fire impingement area), and data at $0.01 < (r^*)^{-0.5461} \times (Q_v^*)^{0.9058} < 0.04$ correspond to the area of $r > 0.18d$ (virtual fire non-impingement area). The data in the $0 < (r^*)^{-0.5461} \times (Q_v^*)^{0.9058} < 0.01$ and $0.01 < (r^*)^{-0.5461} \times (Q_v^*)^{0.9058} < 0.04$ two areas represented two different linear laws. In order to obtain a more suitable prediction model, multiple regression analysis of the experimental results was performed, respectively, at impingement area and non-impingement area as defined by Alpert. The regression model at impingement area and non-impingement area of virtual fire was obtained by the stepwise regression and by rejecting the parameters slightly influencing the model. The experimental results and results of regression model analysis are plotted and shown in Figures 14 and 15, respectively.

At impingement area of virtual fire, the dimensionless virtual fire HRR was the only key parameter obtained through stepwise regression by rejecting the parameters slightly influencing the model. The regression model was written as Equation (38), with RMSE as 0.062 and the adjusted coefficient of determination as 0.96. Equation (38) illustrated that the maximum temperature increase was independent of the parameters except for virtual fire HRR, which was similar to the study of Alpert.

$$\theta^* = 9.713(Q_v^*)^{0.5546} \tag{38}$$

In the non-impingement area of the virtual fire, the regression model could be expressed as Equation (39), with RMSE as 0.27 and the adjusted coefficient of determination as 0.92. The dimensionless distance and virtual fire HRR were still the key parameters for the regression model obtained through stepwise regression.

$$\theta^* = 141.104(r^*)^{-1.3652}(Q_v^*)^{0.8676} \tag{39}$$

Abovementioned analysis indicated that the regional regression was better than the total regression for prediction of the experimental results.

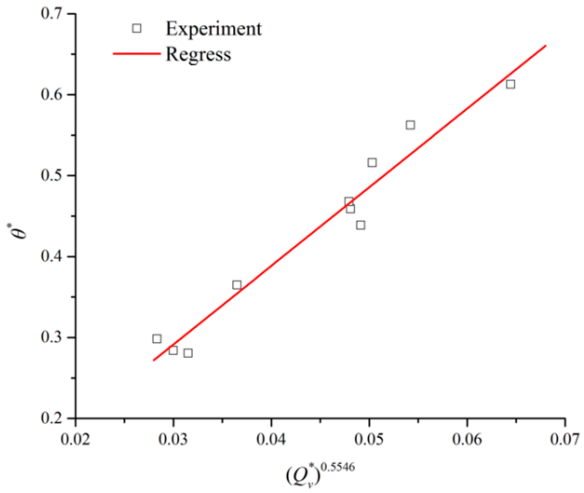

Figure 14. Measured and regression model for estimating the dimensionless maximum temperature increase in the impingement area.

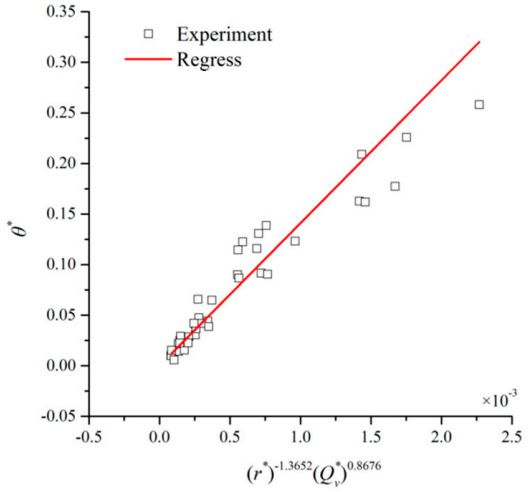

Figure 15. Measured and regression model for estimation of the dimensionless maximum temperature increase in the non-impingement area.

Equations (26) and (28) were substituted in Equations (38) and (39), respectively, and the correlations between average smoke temperature in fire room and the maximum temperature under corridor ceiling could be written as:

$$\theta^* = \begin{cases} 9.713(a_1 y^2 + b_1 y + c_1)^{0.5546}, r \le 0.18d \\ 141.104(r/H)^{-1.3652}(b_2 y + c_2)^{1.3652}(a_1 y^2 + b_1 y + c_1)^{0.8676}, r > 0.18d \end{cases} \quad (40)$$

where the average smoke temperature y in the fire room could be expressed by dimensionless pool fire HRR in the room as Equation (31).

5. Conclusions

This work provides a theoretical analysis of the relationships between maximum smoke temperature beneath the corridor ceiling and the smoke temperature in the fire room. A set of reduced-scale experiments were also performed in this study, taking the heat release rate and the height and width of the corridor into account. The following can be drawn according to this study:

(a) A virtual fire model was proposed to investigate the correlations between the maximum temperature increase under the corridor ceiling and the smoke temperature in the fire room, and based on the Buckingham's theorem and dimensional analysis, we obtained four dimensionless numbers which affect the maximum smoke temperature under the corridor ceiling.

(b) Corridor height had a visible impact on the virtual fire HRR and the position of the virtual fire source. Inversely, the virtual fire HRR and the position of the virtual fire source were insignificantly affected due to the transformation of corridor width.

(c) Quadratic polynomial could be used to describe the relationship between the dimensionless virtual fire HRR and the dimensionless smoke temperature in the room. The dimensionless distance from the virtual fire source to corridor ceiling changed linearly with the dimensionless smoke temperature in the room.

(d) The experimental results indicated that the dimensionless maximum temperature increase declined exponentially with distance. In the impingement area of the virtual fire, the virtual fire HRR could be substituted into the correlation provided by Alpert to predict the maximum temperate increase beneath the corridor ceiling, and the estimated results were in good agreement with the experimental results. In the non-impingement area of the virtual fire, when the virtual fire HRR was substituted into Alpert's correlation, the predicted results were less than the experimental results because smoke was confined by the walls, and it conformed to the restriction of Alpert's correlations. However, the experimental results changed linearly with the predicted results.

(e) The dimensional analysis and multiple regression analysis of the experimental results indicated that the dimensionless viscosity and conduction exhibited an insignificant impact on the dimensionless maximum temperature increase in the corridor. The correlations between the dimensionless maximum temperature increase in the corridor and the dimensionless virtual fire HRR were obtained in the impingement and non-impingement areas of the virtual fire, respectively. In the impingement area of the virtual fire, the dimensionless virtual fire HRR was the only key parameter affecting the dimensionless maximum temperature; in the non-impingement area of the virtual fire, both the dimensionless virtual fire HRR and dimensionless distance were the key parameters affecting the dimensionless maximum temperature.

(f) Based on the correlations between the dimensionless maximum temperature under the corridor ceiling and the virtual fire, by replacing the parameters of the virtual fire with the dimensionless smoke temperature in the room, the model was developed to provide the correlations between the dimensionless maximum temperature increase beneath the corridor ceiling and the dimensionless smoke temperature in the fire room.

Finally, this study provided a simple method to predict the maximum smoke temperature in a corridor. Being subject to the conditions of the experiments, the constants in derived correlations were not universal, and the current approach could be further taken to complement and modify the correlations as follows: Carry out the experiments with a solid fire source in different cases; perform real fire tests in a proper building, and so on. Moreover, this study briefly examined the relationships between the maximum smoke temperature in a corridor and the pool fire HRR in a room. It would be useful to continue studying these correlations more thoroughly.

Acknowledgments

This work was supported by PLA University of Science and Technology.

Author Contributions

Zheli Xing and Jinfeng Mao conceived the study plan. All six authors contributed to the development and analysis of the data and to the writing of the manuscript. All authors read and approved the final manuscript.

Conflicts of Interest

The authors declare no conflict of interest.

Nomenclature

a, b, c, d, n, t, a_1,b_1, c_1, b_2, c_2, a_3, b_3, c_3, b_4, c_4	constant
A	wall area of fire room, m^2
A_o	area of door, $w \times H_o$, m^2
C_d	opening flow coefficient
c_p	specific heat of gas, $kJ \cdot kg^{-1} \cdot k^{-1}$
d	distance from virtual fire source to corridor ceiling, $d = z + (H - H_o)$, m
d^*	dimensionless virtual fire source position, defined by Equation (25)
D	pool diameter, m
g	gravity acceleration, $m \cdot s^{-2}$
h	effective conduction heat transfer coefficient of room, $kW \cdot m^{-2} \cdot K^{-1}$
h^*	dimensionless effective conduction heat transfer coefficient of room, $h^* = \frac{hA}{\rho_\infty c_p A_o \sqrt{gH_o}}$
h_v	effective conduction heat transfer coefficient of corridor, $kW \cdot m^{-2} \cdot K^{-1}$
h_v^*	dimensionless effective conduction heat transfer coefficient of corridor, defined by Equation (15)
H	corridor height, m
ΔH	heat of combustion of fuel, $kJ \cdot kg^{-1}$
H_D	smoke height in room, m
H_N	height of neutral plane, m

H_o	height of door, m
L	length scale
$\dot{m}$	gas mass flow rate, kg·s^{-1}
$\dot{m}_p$	virtual fire plume mass flow rate at the height of z, kg·s^{-1}
m_f	mass loss rate of fire, kg·s^{-1}
$\dot{Q}$	heat release rate of pool fire in room, kW
Q^*	dimensionless heat release rate of pool fire in room, $Q^* = \dfrac{\dot{Q}}{c_p T_\infty \rho_\infty \sqrt{gD} D^2}$
$\dot{Q}_v$	heat release rate of virtual fire, defined by Equation (10), kW
$\dot{Q}_v^*$	dimensionless heat release rate of virtual fire, defined by Equation (14)
r	longitudinal distance from virtual fire, m
r^*	dimensionless longitudinal distance from virtual fire, defined by Equation (13)
R_v^*	Reynolds number, defined by Equation (17)
T_b	smoke temperature in corridor, K
ΔT_g	the difference between virtual fire plume temperature at height of z and environment temperature, K
T_r	smoke layer temperature in room, K
ΔT_r	the difference between smoke layer temperature in room and environment temperature, K
T_∞	environment temperature, K
w	width of door, m
W	corridor width, m
W^*	dimensionless ratio of width to height of corridor, $W^* = W/H$
X_1, X_2, X_3, X_4	standard for the dimensionless number r^*, Q_v^*, H_v^*, R_v^* respectively
y	ratio of room smoke layer temperature to environment temperature, $y = T_r/T_\infty$
z	the distance from virtual fire source to door soffit, m
α	combustion efficiency
μ	dynamic viscosity, N·m·s^{-2}
μ_{20}	value of dynamic viscosity at 20 °C, N·m·s^{-2}
θ	maximum temperature increase in the corridor, $\theta = T_{b,max} - T_\infty$, K
θ_{Alpert}	maximum temperature increase predicted by Alpert correlations, K
θ*	dimensionless maximum temperature increase in the corridor, $\theta^* = \theta/T_\infty$
ρ_r	density of smoke in room, kg·m^{-3}
ρ_∞	density of environment gas in room, kg·m^{-3}
Subscripts	
f	full-scale
in	flow-in of room
m	model-scale
max	maximum
out	flow-out of room

References

1. Alarie, Y. Toxicity of fire smoke. *Crit. Rev. Toxicol.* **2002**, *32*, 259–289.
2. Huo, R.; Hu, Y.; Li, Y.Z. *Introduction to Building Fire Safety Engineering*; China Science and Technology University Press: Hefei, China, 2009; pp. 90–91.
3. Leitner, A. The fire catastrophe in the Tauern Tunnel: Experience and conclusions for the Austrian Guidelines. *Tunn. Undergr. Space Technol.* **2001**, *16*, 217–223.
4. McCaffrey, B.J.; Quintiere, J.G.; Harkleroad, M.F. Estimating room temperatures and the like hood of flashover using fire testdata correlations. *Fire Technol.* **1981**, *17*, 98–119.
5. Sharma, P.; Quintiere, J.G. Compartment fire temperatures. *J. Fire Prot. Eng.* **2010**, *20*, 253–271.
6. Chen, A.P.; Francis, J.; Dong, X.L.; Chen, W.H. An experimental study of the rate of gas temperature rise in enclosure fires. *Fire Saf. J.* **2011**, *46*, 397–405.
7. Quintiere, J.; McCaffrey, B.J.; Kashiwagi, T. A scaling study of a corridor subject to a room fire. *Combust. Sci. Technol.* **1978**, *18*, 1–19.
8. Alpert, R.L. Calculation of response time of ceiling-mounted fire detectors. *Fire Technol*. **1972**, *8*, 181–195.
9. Kurioka, H.; Oka, Y.; Satoh, H.; Sugawa, O. Fire properties in near field of square fire source with longitudinal ventilation in tunnels. *Fire Saf. J.* **2003**, *38*, 319–340.
10. Hu, L.H.; Huo, R.; Wang, H.B.; Li, Y.Z.; Yang, R.X. Experimental studies on fire-induced buoyant smoke temperature distribution along tunnel ceiling. *Build. Environ.* **2007**, *42*, 3905–3915.
11. Hu, L.H.; Huo, R.; Li, Y.Z.; Wang, H.B.; Chow, W.K. Full-scale burning tests on studying smoke temperature and velocity along a corridor. *Tunn. Undergr. Space Technol.* **2005**, *20*, 223–229.
12. Hu, L.H.; Huo, R.; Peng, W.; Chow, W.K.; Yang, R.X. On the maximum smoke temperature under the ceiling in tunnel fires. *Tunn. Undergr. Space Technol.* **2006**, *21*, 650–655.
13. Ji, J.; Zhong, W.; Li, K.Y.; Shen, X.B.; Zhang, Y.; Huo, R. A simplified calculation method on maximum smoke temperature under the ceiling in subway station fires. *Tunn. Undergr. Space Technol.* **2011**, *26*, 490–496.
14. Ji, J.; Fan, C.G.; Zhong, W.; Shen, X.B.; Sun, J.H. Experimental investigation on influence of different transverse fire locations on maximum smoke temperature under the tunnel ceiling. *Int. J. Heat Mass Transf.* **2012**, *55*, 4817–4826.
15. Fan, C.G.; Ji, J.; Gao, Z.H.; Sun, J.H. Experimental study on transverse smoke temperature distribution in road tunnel fires. *Tunn. Undergr. Space Technol.* **2013**, *37*, 89–95.
16. Gao, Z.H.; Ji, J.; Fan, C.G.; Sun, J.H.; Zhu, J.P. Influence of sidewall restriction on the maximum ceiling gas temperature of buoyancy-driven thermal flow. *Energy Build.* **2014**, *84*, 13–20
17. Johansson, N.; van Hees, P. A correlation for predicting smoke layer temperature in a room adjacent to a room involved in a pre-flashover fire. *Fire Mater.* **2014**, *38*, 182–193.
18. Gao, Z.H.; Ji, J.; Fan, C.G.; Sun, J.H. Experimental analysis of the influence of accumulated upper hot layer on the maximum ceiling gas temperature by a modified virtual source origin concept. *Int. J. Heat Mass Transf.* **2015**, *84*, 262–270.
19. Shigunov, V. A zone model for fire development in multiple connected compartments. *Fire Saf. J.* **2005**, *40*, 555–578.
20. Thomas, P.H. Modeling of compartment fires. *Fire Saf. J.* **1983**, *5*, 181–190.

21. Rockett, J.A. Fire induced gas flow in an enclosure. *Combust. Sci. Technol.* **1976**, *12*, 165–175.
22. Heskestad, G. Fire plumes, flame height, and air entrainment. In *The SFPE Handbook of Fire Protection Engineering*, 3rd ed.; National Fire Protection Association: Quincy, MA, USA, 2002; Section 2, Chapter 1.
23. Zukoski, E.E. Properties of Fire Plumes. In *Combustion Fundamentals of Fire*; Cox G., Ed.; Academic Press: London, UK, 1995.
24. Steckler, K.D.; Quintiere, J.G.; Rinkinen, W.J. Flow induced by fire in a compartment. In Proceedings of the National Bureau of Standards, Symposium (International) on Combustion, Gaithersburg, MD, USA, 14–16 September 1982; NBSIR 82-2520.
25. Thomas, P.H. Dimensional analysis: A magic art in fire research? *Fire Saf. J.* **2000**, *34*, 111–141.
26. Wang, L.; Quintiere, J.G. An analysis of compartment fire doorway flows. *Fire Saf. J.* **2009**, *44*, 718–731.
27. Buckingham, E. On physically similar systems: Illustrations of the use of dimensional equations. *Phys. Rev.* **1914**, *4*, 345–376.
28. Tanaka, T.; Yamada, S. Reduced scale experiments for convective heat transfer in the early stage of fires. *Int. J. Eng. Perform. Based Fire Codes* **1999**, *3*, 196–203.
29. Zhao, X.B.; Zhou, X. *Fluid Mechanics with Engineering Applications*; Southeast University Press: Nanjing, China, 2008; p. 11.
30. Karlsson, B.; Quintiere, J.G. *Enclosure Fire Dynamics*; CRC Press: Washington, DC, USA, 2000; pp. 54–60.
31. Babrauskas, V. Heat release rate. In *The SFPE Handbook of Fire Protection Engineering*, 3rd ed.; National Fire Protection Association: Quincy, MA, USA, 2002; Section 3, Chapter 1.
32. Pitts, W.M.; Braun, E.; Peacock, R.D.; Mitler, H.E.; Johnsson, E.L.; Reneke, P.A.; Blevins, L.G. Thermocouple measurement in a fire environment. In *National Institute of Standards and Technology Internal Report*; National Institute of Standards and Technology: Gaithersburg, MD, USA, 1999.
33. Blevins, L.G. Behavior of bare and aspirated thermocouples in compartment fires. In Proceedings of the 33rd National Heat Transfer Conference, Albuquerque, NM, USA, 15–17 August 1999.
34. Alpert, R.L. Ceiling jet flows. In *The SFPE Handbook of Fire Protection Engineering*, 3rd ed.; National Fire Protection Association: Quincy, MA, USA, 2002; Section 2, Chapter 2.
35. Wooldridge, J.M. A note on computing *R*-squared and adjusted *R*-squared for trending and seasonal data. *Econ. Lett.* **1991**, *36*, 49–54.
36. Ying, Z.L.; Ingason, H. The maximum ceiling gas temperature in a large tunnel fire. *Fire Saf. J.* **2012**, *48*, 38–48.